Estimation of Effects of Air Pollution on the Corrosion of Historical Buildings in Bangkok

Nuttacha Daengprathum[1], Rattapon Onchang[1*], Kanchana Nakhapakorn[2], Ornprapa Robert[1], Aungsiri Tipayarom[1], and Peter Johann Sturm[3]

[1]Department of Environmental Science, Faculty of Science, Silpakorn University, Muang, Nakhon Pathom 73000, Thailand
[2]Faculty of Environment and Resource Studies, Mahidol University, Salaya, Nakhon Pathom 73170, Thailand
[3]Institute for Internal Combustion Engines and Thermodynamics, Graz University of Technology, Graz A-8010, Austria

ARTICLE INFO

Received: 17 Mar 2022
Received in revised: 28 May 2022
Accepted: 30 May 2022
Published online: 11 Jul 2022
DOI: 10.32526/ennrj/20/202200071

Keywords:
Air pollution/ Bangkok/ Corrosion/ Geographic information systems (GIS)/ Historical buildings/ Inverse distance weighting (IDW)

*** Corresponding author:**
E-mail: onchang_r@su.ac.th; rattapon.onchang@gmail.com

ABSTRACT

Historical buildings are recognized as the valuable cultural heritage of a nation. They may suffer material deterioration unavoidably because of exposure to air pollution. We used geographic information systems with dose-response functions (DRFs) to estimate the corrosion of copper and Portland limestone, and their risk of corrosion with regard to historical buildings in Bangkok, Thailand. The first step was to find a suitable spatial interpolation method considering the air pollution and meteorological measurement data for 2010-2019 from 26 monitoring stations in Bangkok and its neighborhoods. Applying multiple performance measures, the inverse distance weighting (IDW) method was found to be the most suitable. Predictions of the pollutant concentration in the spatial atmosphere showed that the concentration of all pollutants (SO_2, NO_2, O_3, and PM_{10}) tends to increase in 2028. Air pollution exposure time duration tends to be a key factor affecting the corrosion of material. The results of spatial corrosion estimations indicated that in 2010, the corrosion of copper and Portland limestone were at acceptable levels; however, the estimated corrosion levels for 2019 and 2028 are higher and beyond the acceptable levels. Moreover, both materials in the Rattanakosin historical area exceed their tolerable corrosion rates with considerably serious risks in 2028. The results can be further used to establish active measures to reduce the rate of corrosion of historical buildings in Bangkok.

1. INTRODUCTION

Although historical buildings indicate the historical origin of a nation, they also are a part of international cultural heritage and should be conserved. Many historical buildings suffer damage due to air pollution from various sources such as traffic activities, road and building construction, and industries. Pollutants are deposited and accumulated on the building surface. Under suitable atmospheric conditions of temperature, rainfall, and humidity, these pollutants can corrode the building materials; ancient materials are also affected by exposure time and material type (Barnoos et al., 2020; Richards et al., 2020; El-Gohary and Moneim, 2021). The impact of atmospheric pollution on material corrosion has been investigated for decades. The International Co-operative Program on Effects on Materials including Historic and Cultural Monuments (ICP Materials) and the MULTI-ASSESS project of the United Nations Economic Commission for Europe (UNECE) (Tidblad et al., 2001; Reiss et al., 2004) initially conducted field experiments to observe building material corrosion and measure air pollutants and meteorological parameters. The collected data were analyzed using multiple regression methods to develop dose-response functions (DRFs). DRFs were used to estimate the effect of atmospheric pollution on historical buildings (Christodoulakis et al., 2016; Onchang and Hawker, 2019; Broomandi et al., 2021). Building material deterioration under defined temporal and spatial conditions were estimated using a geographic information system (GIS) with DRFs.

Interpolation methods in GIS (e.g., inverse distance weighting (IDW), spline, and kriging) were used to estimate the spatial contribution of atmospheric pollutants and corrosion of materials in areas of interest (Castillo-Miranda et al., 2017; Eslami and Ghasemi, 2018; Castillo-Miranda et al., 2021). IDW determines

Citation: Daengprathum N, Onchang R, Nakhapakorn K, Robert O, Tipayarom A, Sturm PJ. Estimation of effects of air pollution on the corrosion of historical buildings in Bangkok. Environ. Nat. Resour. J. 2022;20(5):505-514. (https://doi.org/10.32526/ennrj/20/202200071)

values at nearby locations using a linear-weighted combination set of sample points. It provides an option to adjust smoothness of the results by setting power k, which controls the degree of local influence (Chang, 2018). Spline estimates values by minimizing overall surface curvature, resulting in smoothly varying surfaces of the parameters (Childs, 2004). Kriging is based on a geostatistical method for spatial interpolation. Unlike other interpolation methods, it can generate prediction errors to assess the quality of prediction. Kriging relies on the semivariogram, which quantifies spatial autocorrelation in the dataset. The semivariogram fitted with a mathematical function will be used for estimating the semivariance at any given distance. There are several types of kriging; ordinary and universal kriging are the commonly used methods (Chang, 2018).

However, to the best of our knowledge, a limited evaluation process to validate these interpolation methods prior to their application was reported in the previous studies. For example, Spain (De la Fuente et al., 2013) and Turkey (Karaca, 2013) selected the kriging method to interpolate spatial distribution of air pollution with no evaluation of the method, while Castillo-Miranda et al. (2021) used root means square as a single indicator to select the two methods-IDW and kriging-for mapping of the contribution of nitric acid to atmospheric corrosion on zinc material. Thus, this possibly raises questions regarding the validity of the results.

Bangkok was ranked as the world's number one tourist destination in 2018 by the Mastercard Global Destination Cities Index, with the number of tourists reaching 22.78 million in 2018 (Mastercard, 2019). The ancient religious monuments located in the historical Rattanakosin area in Bangkok are popular tourist destinations. However, according to the United Nations Environment Program (UNEP), Bangkok is an urban area plagued by air pollution over the years (UNEP, 2019). The high degree of air pollution, causing corrosion of the monuments in Bangkok, seems unavoidable. This, in turn, affects tourism in the long run.

This study aimed to assess material corrosion throughout Bangkok and its historical area (Rattanakosin) using GIS with DRFs. Statistical analysis was applied for selecting interpolation methods. The spatiotemporal impacts of atmospheric pollution on the monument materials were identified. The results can be used to formulate suitable conservation and restoration plans for the historical buildings.

2. METHODOLOGY

2.1 Data collection

2.1.1 Spatial data

Digital topographic maps of Bangkok, collected from Bangkok Metropolitan Administration GIS Center, were based on the Universal Transverse Mercator (UTM) with World Geodetic System (WGS) 1984 Zone 47. Geographic coordinates of the Buddhist monuments in the Rattanakosin historical area, registered as ancient monuments in the Royal Thai Government Gazettes for 1949-2009 (Ministry of Culture, 2017), were collected from the Fine Arts Department, Ministry of Culture. These monuments are located in 12 Buddhist temples. Coordinates of air quality monitoring stations in Bangkok and its neighborhood (total: 26 stations) were received from the Pollution Control Department of Thailand (PCD) (Figure 1).

2.1.2 Attribute data

Data of monument names and construction materials were obtained from the Fine Arts Department. Annual air quality and meteorological data (2010-2019), comprising air pollutant (SO_2, NO_2, O_3, and PM_{10}) concentrations, temperature, relative humidity, and precipitation amount from the 26 stations, were collected from the PCD. H^+ concentrations in precipitation were received from the database of Acid Deposition Monitoring Network in East Asia (EANET).

2.2 Dose-response functions

Multipollutant DRFs obtained from ICP Materials and the MULTI-ASSESS project of UNECE (European Union, 2005; Kucera, 2014) were used to estimate the deterioration rates of copper and Portland limestone (Table 1), which are commonly used in the monuments (Karaca, 2013; Onchang and Hawker, 2019). DRFs were previously used to examine the building material deterioration world-wide (Broomandi et al., 2021). Since DRFs are provided on an annual basis, all air pollutant and meteorological data were gathered on an annual basis. Deterioration rates can be expressed as either material loss (ML) (g/m^2) or surface recession (R) (μm). R can be obtained by dividing ML by material density (g/cm^3).

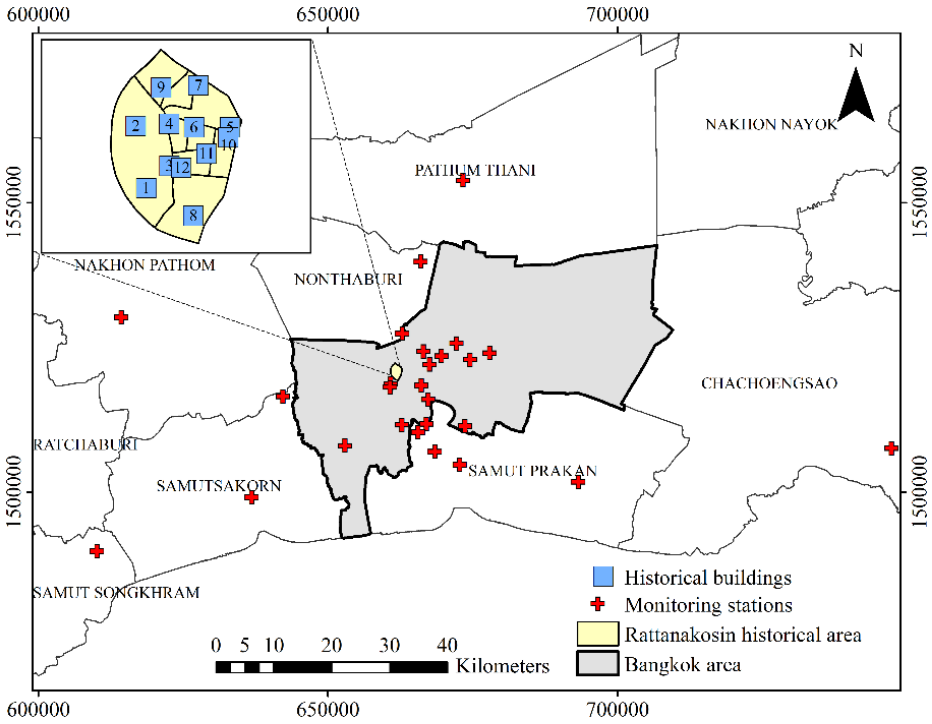

Figure 1. Study area: Bangkok and its surrounding provinces

Note: Numbers in the Rattanakosin historical area indicate the Buddhist historical buildings in the following temples: (1) Wat Phra Chettuphon Wimon Mangkhalaram; (2) Wat Mahathat Yuwarajarangsarit Rajaworamahavihara; (3) Wat Ratchapradit Sathitmahasimaram; (4) Wat Buranasiri Matayaram; (5) Wat Ratchanatdaram; (6) Wat Mahannapharam; (7) Wat Bowonniwet Wihan Ratchaworawihan; (8) Wat Rat Burana Ratchaworawihan; (9) Wat Chana Songkhram Ratchawora Maha Wihan; (10) Wat Thep Thidaram Woraviharn; (11) Wat Suthat Thepwararam Ratchaworamahawihan; and (12) Wat Ratchabophit Sathitmahasimaram Ratchaworawihan

Table 1. Dose-response functions (DRFs) for multipollutant situations and temperature functions of unsheltered copper and Portland limestone

Material	Dose-response function (DRF)	Temperature function
Copper[a]	$ML = 3.12 + \{1.09 + 0.00201[SO_2]^{0.4}[O_3]Rh_{60}e^{f(T)} + 0.0878Rain[H^+]\}t$	$f(T) = -0.032(T-10)$ (when $T \geq 10°C$)
Portland limestone[b]	$R = 4.0 + 0.0059[SO_2]RH_{60} + 0.054Rain[H^+] + 0.078[HNO_3]Rh_{60} + 0.0258PM_{10}\} t$	

Note: ML is material loss (g/m^2); R is surface recession (µm); $[SO_2]$, $[NO_2]$, $[O_3]$, and $[PM_{10}]$ are the concentrations of these air pollutants in $\mu g/m^3$; Rh is relative humidity (%) (Rh_{60}, which is equal to (Rh-60) when Rh>60 and 0 otherwise); Rain is the cumulative amount of precipitation (mm) over the exposure period (t) (years); (H^+) is the concentration of H^+ in the precipitation (mg/L); t is duration of exposure in years; T is the temperature in °C. The annual HNO_3 concentrations ($\mu g/m^3$) were calculated as $HNO_3 = 516\ e^{-3400/(T+273)} \times ([NO_2][O_3]Rh)^{0.5}$. [a]European Union (2005); [b]Kucera (2014).

2.3 Tolerable corrosion rate

The tolerable corrosion rate (Table 2) is the value representing the technical and economic considerations for a particular material and application for its annual restoration work (Kucera, 2014). It was introduced in the MULTI-ASSESS project by considering two main factors: (1) tolerable corrosion before action based on the stage of deterioration when the restoration starts; and (2) the tolerable time between maintenance based on how often it is acceptable to restore the object. The tolerable corrosion rate (K_{tol}) can be calculated as a multiple (n) of the background corrosion rate:

$$K_{tol} = n \times K_b \quad (1)$$

Where; n is a factor, and K_b is the background corrosion rate.

The corrosion rates of the two materials calculated from DRFs in this current study were compared with their tolerable corrosion rates. The selection of n (Table 2) to analyze the acceptable corrosion rates is important. If n is too high or low, the calculated tolerable corrosion rate value may be higher or lower than the actual value. The tolerable corrosion rate chosen in this study was 2.5 (n=2.5), as it corresponds to the target for protecting the basic structural materials and monuments for 2020 of the ICP Materials Project (UN ECE, 2009) and was also used in previous studies (De la Fuente et al., 2013; Karaca, 2013). Note that the tolerable corrosion rates

used in this study are based on the European context. Thus, using this approach for other areas raises the concern of uncertainty in the results.

Table 2. Tolerable corrosion rates (μm/year) for n=1.0 (background corrosion rate), 1.5, 2.0, and 2.5

Material	n=1.0	n=1.5	n=2.0	n=2.5
Copper	0.32	0.50	0.64	0.80
Portland limestone	3.2	5.0	6.4	8.0

Source: Kucera (2014)

2.4 Mapping

2.4.1 Evaluation of spatial interpolation methods

We used ArcMap version 10.1 software to generate a GIS-based spatial distribution of air pollution and material corrosion in Bangkok. Initially, we validated the estimation of the spatial distribution of air pollutants by four spatial interpolation methods-IDW, spline, ordinary kriging, and universal kriging. The estimated pollutant concentrations were compared with the measured ambient air quality data averaged over all the monitoring stations. For comparison, the following statistical indicators were used: (1) fractional bias (FB)-a measure of the mean relative bias, indicating only systematic errors, and the arithmetic difference between the estimated and observed values; (2) geometric mean bias (MG)-an index for determining the overestimation or underestimation or scatter; (3) normalized mean square error (NMSE)-an estimator of the overall deviation between the estimated and measured values; (4) geometric variance (VG)-factor representing the scatter of the estimated values; (5) correlation coefficient (R)-a measure of how well the estimated values follow trends in measured values; (6) fraction of predictions within a factor of two of estimations (FAC2)-representing the estimation scatter of the spatial estimation method (Dixon and Venkatesh, 2016). The interpolation methods are validated if MG, VG, R, and FAC2 are close to 1, and FB and NMSE are close to 0. These statistical performance measures can be expressed as follows:

$$FB = \frac{\overline{C_o} - \overline{C_p}}{0.5\,(\overline{C_o} + \overline{C_p})} \quad (2)$$

$$MG = \mathrm{Exp}\,(\overline{\ln C_o} - \overline{\ln C_p}) \quad (3)$$

$$NMSE = \frac{\overline{(C_o - C_p)^2}}{\overline{C_o}\,\overline{C_p}} \quad (4)$$

$$VG = \mathrm{Exp}\,[\overline{(\ln C_o - C_p)^2}] \quad (5)$$

$$R = \frac{\overline{(C_o - \overline{C_o})(C_p - \overline{C_p})}}{\sigma_{C_p}\sigma_{C_o}} \quad (6)$$

$$\text{FAC2=the fraction of data that satisfies } 0.5 \le \frac{C_p}{C_o} \le 2.0 \quad (7)$$

Where; C_o is the measured value; C_p, the estimated valued; $\overline{C}_o$, the average of the measured values; $\overline{C}_p$, the average of the estimated valued; σ_{C_o}, the standard deviation of the measured value; and σ_{C_p}, the standard deviation of the estimated value.

2.4.2 Spatial corrosion analysis of historical buildings

The estimated material corrosions were quantified using DRFs (in Table 1) with air pollutants and meteorological input parameters obtained from the monitoring stations in 2010 and 2019. Future corrosion in 2028 was predicted. We projected the values of future pollution and meteorological parameters from the observed data for 2010-2019 using exponential triple smoothing in Microsoft Excel (version 2016) (Microsoft, 2021). Then, we interpolated the obtained corrosion values using the suitable spatial interpolation method selected based on the results of statistical analyses.

3. RESULTS AND DISCUSSION

3.1 Appropriate spatial estimation methods

The validation assessment results of spatial air pollution interpolation methods are listed in Table 3. As each indicator has advantages and disadvantages, multiple performance indicators should be considered in the validation exercise. The overall results in Table 3 suggest that IDW is the appropriate method. FB and MG indicate IDW has lower relative bias and systematic error. NMSE and VG show that IDW has lower systematic and unsystematic (random) errors. FAC2 is probably the most robust because it is not overly influenced by outliers (Chang and Hanna, 2004); it also indicates that IDW performs better than other methods. Our finding agrees with Vorapracha et al. (2015) who evaluated three spatial interpolation methods-IDW, ordinary kriging, and universal kriging-with observed PM_{10} (particulate matter: ≤10 μm) concentrations using root mean square error as the statistical measure. The IDW method was commonly used for spatial air pollution estimation (Jumaah et al., 2019; Pharasit and Chaiyakam, 2019). Therefore, we

selected the IDW method to spatially estimate the corrosion of historical building materials unlike previous studies such as those of De la Fuente et al. (2013) and Karaca (2013), who used ordinary kriging without considering statistical indications.

Table 3. Results of the statistical analyses for evaluating interpolation methods

Air pollutants	Interpolation method	FB	MG	NMSE	VG	R	FAC2
SO_2	IDW	-0.05*	0.96*	0.01*	1.01*	0.14	1.05*
	Spline	-0.11	1.39	0.49	5.31	0.00	1.11
	Kriging (Ordinary)	-0.16	0.87	0.06	1.04	0.15	1.17
	Kriging (Universal)	-0.38	0.80	0.27	1.10	0.16*	1.30
NO_2	IDW	0.05	1.05	0.00*	1.00*	0.07	0.95
	Spline	0.30	-	1.06	-	-0.03	0.74
	Kriging (Ordinary)	-0.02*	0.99*	0.01	1.01	0.20*	1.02*
	Kriging (Universal)	-0.03	0.98	0.02	1.02	0.07	1.03
O_3	IDW	-0.05*	0.95*	0.01*	1.01*	0.06	1.05*
	Spline	-0.20	-	0.63	-	0.03	1.22
	Kriging (Ordinary)	-0.11	0.90	0.02	1.02	0.07	1.11
	Kriging (Universal)	-0.34	0.73	0.17	1.17	0.09*	1.41
PM_{10}	IDW	0.10*	1.21	0.08*	1.43	0.08*	0.91*
	Spline	-0.23	0.93*	0.36	1.50	0.02	1.26
	Kriging (Ordinary)	0.15	1.25	0.09	1.32*	0.00	0.86
	Kriging (Universal)	0.18	1.37	0.13	1.73	0.03	0.83

Note: (*) indicates the best method and (-) represents missing statistical values.

3.2 Spatial estimation of air pollutant concentrations

The interpolation of air pollutant concentrations derived from the IDW method in Bangkok in 2010 and 2019 are shown in Figures 2-5. A comparison of the air pollutant concentrations in these two years showed that the concentrations of all pollutants, except PM_{10}, decreased. The reductions in NO_2 and SO_2 may be attributed to the improvements in vehicle technologies and fuel quality (Holnicki et al., 2021). Because NO_2 is one of the primary air pollutants forming O_3, a decrease in NO_2 is likely related to the reduction in O_3 (Lee et al., 2021; Phonphinyo and Sakunkoo, 2021). The reductions in SO_2, NO_2, and O_3 concentrations during these two years agrees with the reported air quality data for Bangkok (PCD, 2020). The increment in PM_{10} may be related to the rise in construction activities, e.g., the construction of condominiums and sky train lines in Bangkok and its neighborhood. Sanecharoen et al. (2019) reported that the Landsat satellite images for 2008-2014 indicate land-use changes in Bangkok. They discovered that natural areas were being replaced by artificial objects, as indicated by increasing number and density of high-rise buildings in the city. Interestingly, the higher air pollution zone found in the western part of Bangkok indicates the possible influence of fuel combustion in industries in Samut Sakhon province (Department of Industrial Works, 2021).

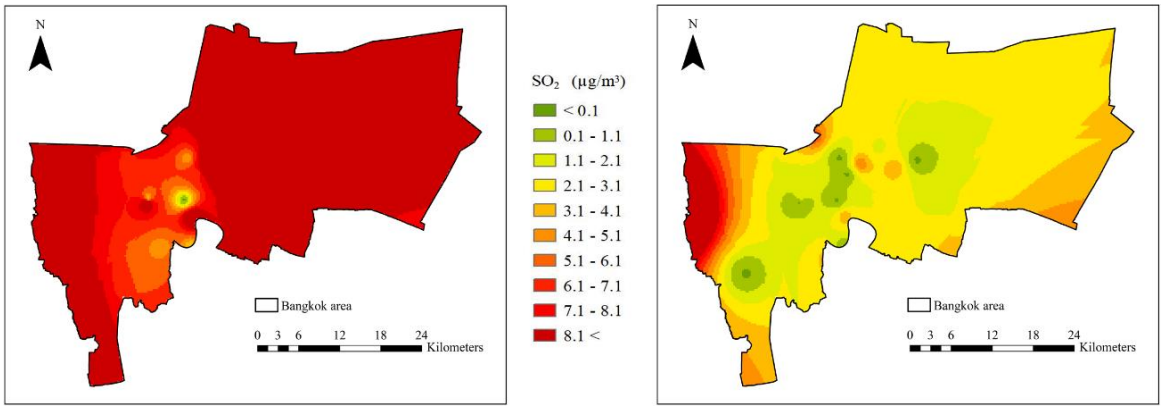

Figure 2. SO_2 concentrations in the study area in 2010 (left) and 2019 (right)

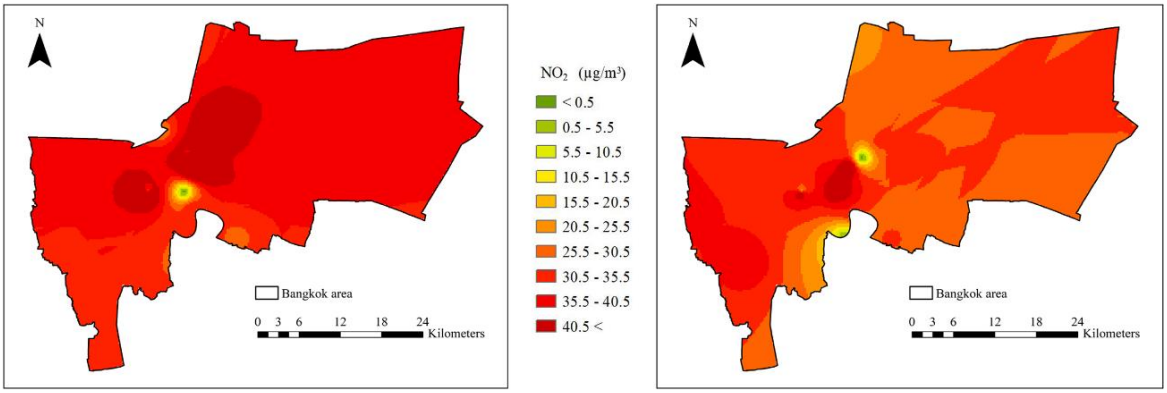

Figure 3. NO_2 concentrations in the study area in 2010 (left) and 2019 (right)

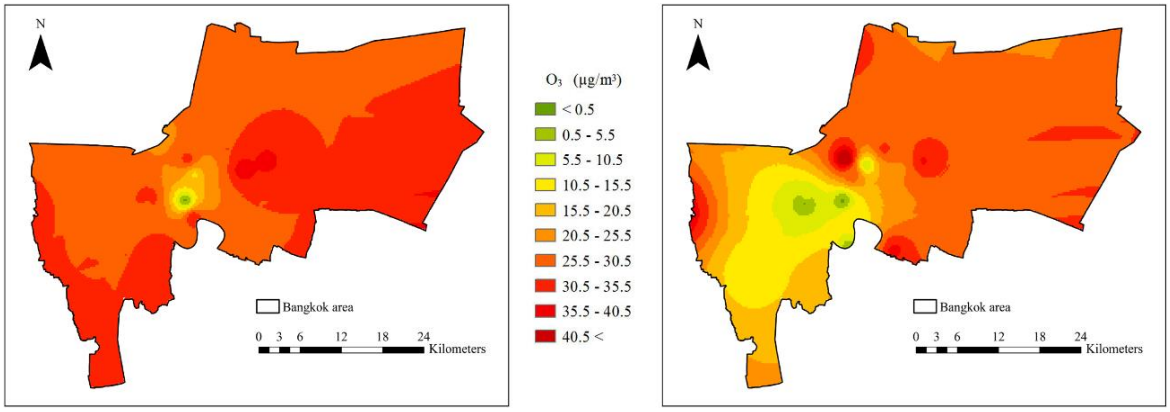

Figure 4. O_3 concentrations in the study area in 2010 (left) and 2019 (right)

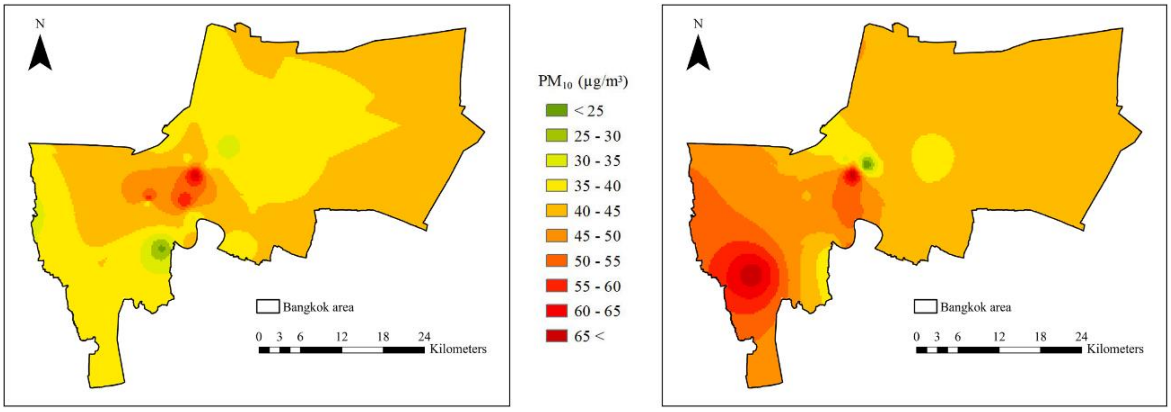

Figure 5. Particulate matter (size ≤10 µm; PM_{10}) concentrations in the study area in 2010 (left) and 2019 (right)

3.3 Corrosion of building materials

The estimated corrosions of copper and Portland limestone in 2010 and 2019 are shown in Figures 6 and 7, respectively. Both materials underwent lower corrosion in 2010 than in 2019. Interestingly, the decrease in the concentrations of air pollutants, namely, SO_2, NO_2, and O_3, were seen with the increase in corrosion rates. This is due to the duration of exposure time, which plays an important role affecting the corrosion as seen in the DRFs (Table 1). Other factors including precipitation, relative humidity and temperature were also responsible for the corrosion. However, this study found their changes over the years were minor. The density of buildings and industries in the area indirectly affect the corrosion of materials. Recently, a study reported the influence of building and industrial densities on land surface temperature in Bangkok (Sanecharoen et al., 2019). As seen from the DRFs (Table 1), temperature plays an important role

in material recession and is used as a variable to explain material corrosion.

The prediction results of air pollution and meteorological parameters for corrosion forecast in 2028 are as follows: air pollution (SO_2, 8 µg/m^3; NO_2, 29 µg/m^3; O_3, 29 µg/m^3; PM_{10}, 44 µg/m^3; and HNO_3, 1.5 µg/m^3); meteorology (temperature, 27.2°C; relative humidity, 70.9%; precipitation, 658.1 mm; and H^+ in the precipitation, 3.04 mg/L). The corrosion forecasts for 2028 (Figure 8) for both materials are much higher than the corrosion estimates for 2010 and 2019 (Figures 6 and 7).

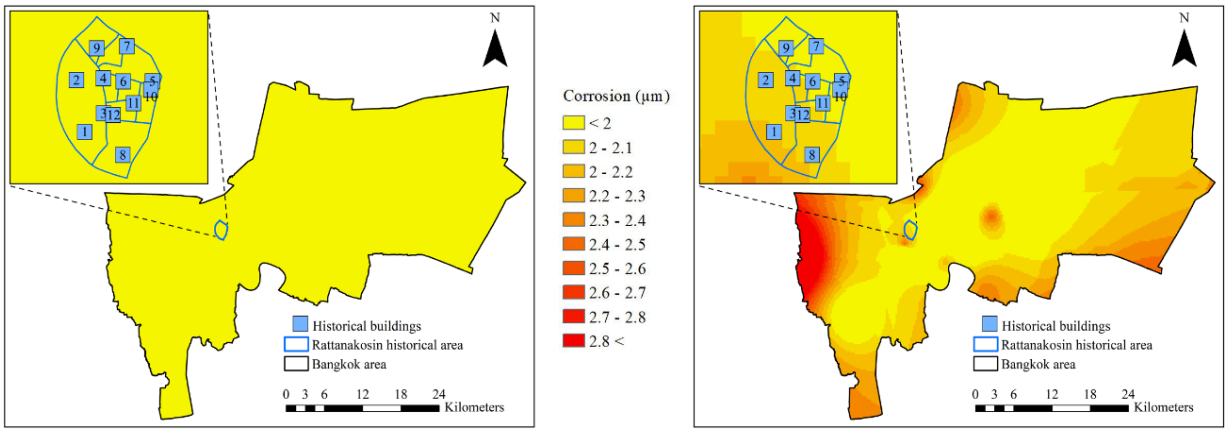

Figure 6. Corrosion of copper in the study area in 2010 (left) and 2019 (right)

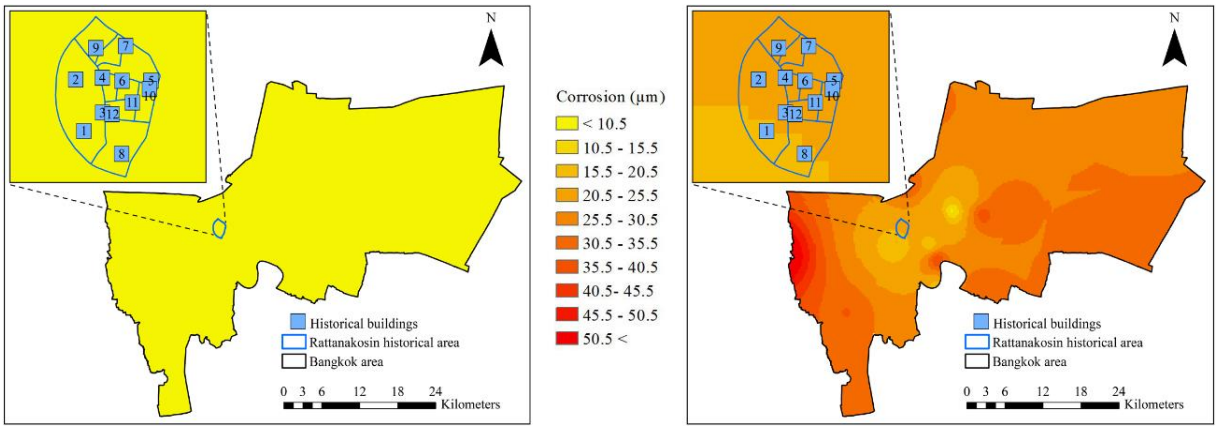

Figure 7. Corrosion of Portland limestone in the study area in 2010 (left) and 2019 (right)

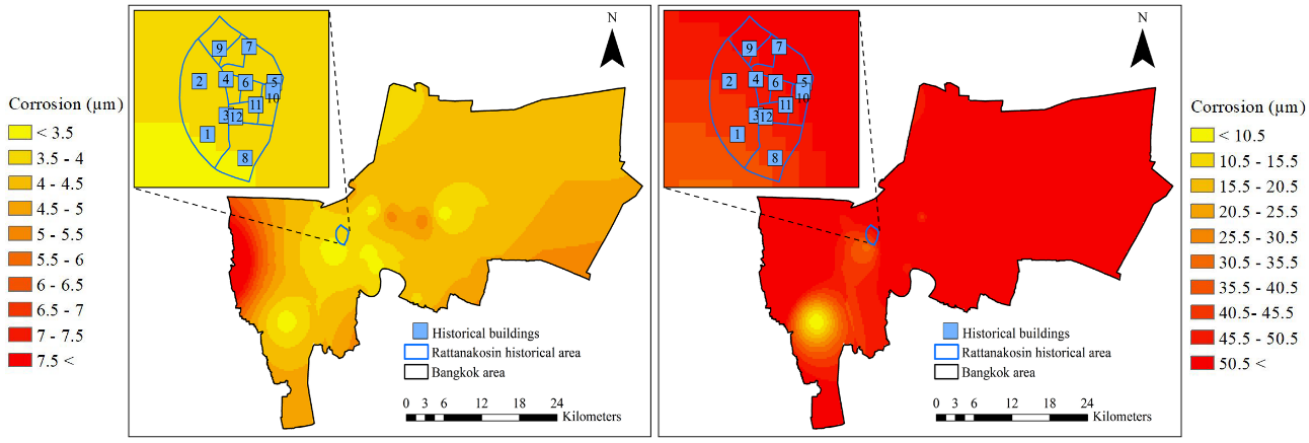

Figure 8. Corrosion of copper (left) and Portland limestone (right) in 2028

The corrosion of the two materials in 2010, 2019, and 2028 with their corresponding tolerable corrosion rates are listed in Table 4. The average corrosion rates of the two materials exceeded their tolerable corrosion rates in 2019 and 2028. The difference between the estimated and tolerable corrosion rates is much larger for Portland limestone than for copper. Overall, the results suggest an urgent need for air pollution mitigation together with measures to prevent building material corrosion both in the current and future situations. Table 4 presents a comparison of the average corrosion rates for copper and Portland limestone in this study for Bangkok with those reported for other cities. For 2010, Bangkok exhibited a lower average corrosion rate for copper and higher average corrosion rate for Portland limestone compared to Istanbul, Turkey. The concentrations of all pollutants (except O_3) and relative humidity in Istanbul were higher those in Bangkok, while the temperature and H^+ concentration in precipitation were lower in Istanbul (Karaca, 2013).

Table 4. Comparison of case studies on monument corrosion

Case study	Year	Material	Corrosion (μm)			
			Minimum	Maximum	Average	Standard deviation
Current study	2010	Copper	0.5	1.0	0.6	<0.1
		Portland limestone	5.8	9.7	7.4	0.3
Current study	2019	Copper	1.6	3.9	2.1	0.3
		Portland limestone	10.4	58.4	29.8	4.7
Current study	2028	Copper	3.3	10.7	4.4	0.8
		Portland limestone	6.8	220.9	67.3	20.1
Madrid[a]	2010	Copper	-	-	-	-
		Portland limestone	4.4	5.2	-	-
Istanbul[b]	2010	Copper	0.8	2.1	1.1	0.3
		Portland limestone	4.0	7.6	5.2	0.7
			Tolerable corrosion rates (μm)[c]			
		Copper	0.8			
		Portland limestone	8.0			

Note: [a]De la Fuente et al. (2013), [b]Karaca (2013), and [c]referred to the values in Table 2

Considering the DRF of copper (Table 1), the air pollutants and relative humidity in Istanbul may exhibit a stronger effect on the corrosion of copper than the conditions in Bangkok. The corrosion risk for Portland limestone is higher in Bangkok than in Istanbul. Similar to the above interpretation, the DRF variables, including temperature, H^+ concentration in precipitation, and calculated HNO_3 concentrations are higher for Bangkok than for Istanbul. Hence, these parameters may demonstrate a greater effect on the corrosion of Portland limestone in Bangkok. Note that in the Istanbul case study (Karaca, 2013), the cumulative amount of precipitation was not considered; hence, this variable was excluded in this comparison.

3.4 Corrosion of monuments in the Rattanakosin historical area

Estimates of the material corrosion in the Rattanakosin historical area are listed in Table 5. A comparison of the estimates for 2019 and 2028 shows that the corrosion rates of all monuments increased and exceeded the tolerable corrosion rates of the materials.

For copper, the highest risk in 2019 corresponded to the monument in temple No. 1 (2.1-2.2 μm), and more serious risks in 2028 correspond to more monuments (temples No. 2-7 and 9-12), with corrosion rates of 3.5-4.0 μm. For Portland limestone, the corrosion rates in 2019 and 2028 far exceeded its tolerable corrosion rate (8.0 μm). The highest risks were in the range of 20.5-25.5 μm in 2019 and exceeded 50.5 μm in 2028.

Note that the estimation accuracy of corrosion risk depends on many factors, such as building damage directionality considering the current exposure conditions, material composition, structural features of different ancient sites, and validity of DRFs under different atmospheric conditions. More research is required to consider these factors.

Table 5. Analysis of the corrosion risk of the historical monuments in the study area

No.	Temple	Material	Corrosion (µm)		
			2010*	2019**	2028**
1	Wat Phra Chettuphon Wimon Mangkhalaram	Copper	0.6-0.7	2.1-2.2	<3.5
		Portland limestone	7.0-7.4	15.5-20.5	35.5-45.5
2	Wat Mahathat Yuwarajarangsarit Rajaworamahavihara	Copper	0.6-0.7	2.0-2.1	3.5-4.0
		Portland limestone	7.0-7.4	20.5-25.5	45.5-50.5
3	Wat Ratchapradit Sathitmahasimaram	Copper	0.6-0.7	2.0-2.1	3.5-4.0
		Portland limestone	7.0-7.4	20.5-25.5	40.5-45.5
4	Wat Buranasiri Matayaram	Copper	0.6-0.7	2.0-2.1	3.5-4.0
		Portland limestone	7.0-7.4	20.5-25.5	45.5-50.5
5	Wat Ratchanatdaram	Copper	0.6-0.7	<2.0	3.5-4.0
		Portland limestone	7.0-7.4	20.5-25.5	>50.5
6	Wat Mahannapharam	Copper	0.6-0.7	<2.0	3.5-4.0
		Portland limestone	7.0-7.4	20.5-25.5	45.5-50.5
7	Wat Bowonniwet Wihan Ratchaworawihan	Copper	0.6-0.7	<2.0	3.5-4.0
		Portland limestone	7.0-7.4	20.5-25.5	>50.5
8	Wat Rat Burana Ratchaworawihan	Copper	0.6-0.7	2.0-2.1	<3.5
		Portland limestone	7.0-7.4	15.5-20.5	40.5-45.5
9	Wat Chana Songkhram Ratchawora Maha Wihan	Copper	0.6-0.7	<2.0	3.5-4.0
		Portland limestone	7.0-7.4	20.5-25.5	45.5-50.5
10	Wat Thep Thidaram Woraviharn	Copper	0.6-0.7	<2.0	3.5-4.0
		Portland limestone	7.0-7.4	20.5-25.5	>50.5
11	Wat Suthat Thepwararam Ratchawora Mahawihan	Copper	0.6-0.7	<2.0	3.5-4.0
		Portland limestone	7.0-7.4	20.5-25.5	45.5-50.5
12	Wat Ratchabophit Sathitmahasimaram Ratchaworawihan	Copper	0.6-0.7	2.0-2.1	3.5-4.0
		Portland limestone	7.0-7.4	20.5-25.5	45.5-50.5
			Tolerable corrosion rates (µm)[a]		
		Copper	0.8		
		Portland limestone	8.0		

Note: *Since the estimation results did not show the differences among the monuments in the year 2010 (Figure 6 left and Figure 7 left), the annual corrosion of copper and Portland limestone were in the range of 0.6-0.7 and 7.0-7.4 µm, respectively. **is the corrosion rate higher than the tolerable corrosion rate of copper material and Portland limestone (0.8 and 8.0 µm, respectively, in Table 2). Underlines are the highest corrosion rates found in the individual year. [a]refers to the values in Table 2

4. CONCLUSION

The appropriate GIS-based interpolation method to reproduce the spatial distribution of ambient air pollution was identified as IDW from the results of statistical analyses. In Bangkok, the concentrations of all pollutants, except PM_{10}, decreased from 2010 to 2019. However, the prediction shows that all pollutants return to increase in 2028. We utilized DRFs with IDW to calculate the spatial corrosion rates of copper and Portland limestone in 2010, 2019, and 2028. The material corrosion rates increased and exceeded their tolerable corrosion rates in 2019 and 2028. Air pollution concentrations together with the duration of exposure time affects the material corrosions. The corrosion rates of monument materials increased beyond their tolerable limit in the Rattanakosin historical area in Bangkok. The results of the current study can serve as concrete information to initiate strategic actions to conserve historical buildings.

ACKNOWLEDGEMENTS

We acknowledge the Pollution Control Department of Thailand (PCD) for the support of air pollution and meteorological data. This research and innovation activity is funded by National Research Council of Thailand (NRCT) and Faculty of Science, Silpakorn University.

REFERENCES

Barnoos V, Oudbashi O, Shekofteh A. The deterioration process of limestone in the Anahita Temple of Kangavar (West Iran). Heritage Science 2020;8(66):1-19.

Broomandi P, Tleuken A, Zhaxylykov S, Nikfal A, Kim JR, Karaca F. Assessment of potential benefits of traffic and urban mobility reductions during COVID-19 lockdowns: Dose-

response calculations for material corrosions on built cultural heritage. Environmental Science and Pollution Research 2021;29(5):6491-510.

Castillo-Miranda JO, Torres-Jardon R, Garcia-Reynoso JA, Mar-Morales BE, Rodriguez-Gomez FJ, Ruiz-Ruarez LG. Mapping recession risk for cultural heritage stone in Mexico City due to dry and wet deposition of urban air pollutants. Atmósfera 2017;30(3):189-207.

Castillo-Miranda JO, Rodriguez-Gomez FJ, Genesca-Llongueras J, Ruiz-Suarez LG, Garcia-Reynoso JA. Estimation and mapping of the contribution of nitric acid to atmospheric corrosion of zinc. Global Journal of Environmental Science and Management 2021;7(4):523-42.

Chang JC, Hanna SR. Air quality model performance evaluation. Meteorology and Atmospheric Physics 2004;87:167-96.

Chang KT. Introduction to Geographic Information Systems. 9th ed. New York: McGraw-Hill Education; 2018.

Christodoulakis J, Tzanis CG, Varotsos CA, Ferm M, Tidblad J. Impacts of air pollution and climate on materials in Athens, Greece. Atmospheric Chemistry Physics Discussions 2016; 17(1):1-27.

Childs C. Interpolating surfaces in ArcGis spatial [Internet]. 2004 [cited 2022 May 14]. Available from: https://www.esri.com/news/arcuser/0704/files/interpolating.pdf.

De la Fuente D, Vega JM, Viejo F, Diaz I, Morcillo M. Mapping air pollution effects on atmospheric degradation of cultural heritage. Journal of Cultural Heritage 2013;14(2):138-45.

Department of Industrial Works. Factory information for officials [Internet]. 2021 [cited 2022 Jan 20]. Available from: http://reg.diw.go.th/executive/Prov3.asp?prov=74.

Dixon B, Venkatesh U. GIS and Geocomputation for Water Resource Science and Engineering. 1st ed. UK: John Wily and Sons Ltd; 2016.

El-Gohary MA, Moneim AA. The environmental factors affecting the archaeological buildings in Egypt, "II Deterioration by severe human activities". Periodico Di Mineralogia 2021; 90(2):41-55.

Eslami A, Ghasemi SM. Determination of the best interpolation method in estimating the concentration of environmental air pollutants in Tehran City in 2015. Journal of Air Pollution and Health 2018;3(4):187-98.

Holnicki P, Nahorski Z, Kaluszko A. Impact of vehicle fleet modernization on the traffic-originated air pollution in an urban area: A case study. Atmosphere 2021;12(12):Article No. 1581.

Jumaah HJ, Ameen MH, Kalantar B, Rizeei HM, Jumaah SJ. Air quality index prediction using IDW geostatistical technique and OLS-based GIS technique in Kuala Lumpur, Malaysia. Geomatics, Natural Hazards and Risk 2019;10(1):2185-99.

Karaca F. Mapping the corrosion impact of air pollution on the historical peninsula of Istanbul. Journal of Cultural Heritage 2013;14(2):129-37.

Kucera V. Chapter VI: Mapping of effects on materials. In: Kucera V, editor. Manual on Methodologies and Criteria for Modeling and Mapping Critical Loads and Levels and Air Pollution Effects, Risks and Trends. Berlin: Federal Environmental Agency (Umweltbundesamt); 2014. p. 1-16.

Lee HJ, Chang LS, Jaffe DA, Bak J, Liu X, Abad GG, et al. Ozone continues to increase in East Asia despite decreasing NO_2: Causes and Abatements. Remote Sensing 2021;13(11):1-17.

Mastercard. Global destination cities index [Internet]. 2019 [cited 2021 Aug 31]. Available from: https://newsroom.mastercard.com/wp-content/uploads/2019/09/GDCI-Global-Report-FINAL-1.pdf.

Microsoft. Forecast.ets function [Internet]. 2021 [cited 2021 Oct 31]. Available from: https://support.microsoft.com/en-us/office/forecast-ets-function-15389b8b-677e-4fbd-bd95-21d464333f41.

Ministry of Culture. Attachment of Act on Ancient Monuments, Antiques, Objects of Art and National Museums (No.2), B.E. 2535: Volume 109. Bangkok: Office of Archaeology, Fine Arts Department; 2017. (in Thai).

European Union. Model for Multi-Pollutant Impact and Assessment of Threshold Levels for Cultural Heritage: EU 5FP RTD Project. Stockholm, Sweden: MULTI- ASSESS Publishable Final; 2005.

Onchang R, Hawker DW. A computational program for estimating atmospheric corrosion of monuments. Environment and Natural Resources Journal 2019;17(3):19-28.

Pharasit M, Chaiyakarm T. Geoinformatics application on air quality assessment: A case study in Bangkok. Thai Science and Technology Journal 2019;28(5):744-58.

Phonphinyo S, Sakunkoo P. The amount of ambient ozone and nitrogen dioxide that relate with traffic around Bueng Srithan in Khon Kaen University area. Research and Development Health System Journal 2021;14(2):135-43.

Pollution Control Department (PCD). Thailand State of Pollution Report 2019. Bangkok, Thailand: PCD; 2020.

Reiss D, Rihm B, Thoni C, Faller M. Mapping stock at risk and release of zinc and copper in Switzerland: Dose response functions for runoff rates derived from corrosion rate data. Water, Air, and Soil Pollution 2004;159:101-13.

Richards J, Bailey R, Mayaud J, Viles H, Guo Q, Wang X. Deterioration risk of dryland earthen heritage sites facing future climatic uncertainty. Scientific Reports 2020;10(1):1-9.

Sanecharoen W, Nakhapakorn K, Mutchimwong A, Jirakajohnkool S, Onchang R. Assessment of urban heat island patterns in Bangkok metropolitan area using time: Series of LANDSAT thermal infrared data. Environment and Natural Resources Journal 2019;17(4):87-102.

Tidblad J, Kucera V, Mikhailov AA, Henriksen J, Kreislova K, Yates T, et al. UN ECE ICP materials: Dose-response functions on dry and wet acid deposition effects after 8 years of exposure. Water, Air, and Soil Pollution 2001;130,1457-62.

United Nations Economic Commission for Europe (UN ECE). Executive body for the convention on long-range transboundary air pollution [Internet]. 2009 [cited 2020 Jan 12]. Available from: https://www.unece.org/fileadmin/DAM/env/documents/2009/EB/wge/ece.eb.air.wg.1.2009.16.e.pdf.

United Nations Environment Programme (UNEP). Air pollution is choking Bangkok, but a solution is in reach [Internet]. 2019 [cited 2020 Jan 12]. Available from: https://www.unep.org/news-and-stories/story/air-pollution-choking-bangkok-solution-reach.

Vorapracha P, Phonprasert P, Khanaruksombat S, Pijarn N. A comparison of spatial interpolation methods for predicting concentrations of particle pollution (PM_{10}). International Journal of Chemical, Environmental and Biological Sciences 2015;3(4):302-6.